THE JOURNAL OF PHYSICAL CHEMISTRY C

Feature Article

pubs.acs.org/JPCC

Molecular Insights in the Structure and Layered Assembly of Polyelectrolytes at the Oil/Water Interface

Ellen J. Robertson and Geraldine L. Richmond*

Department of Chemistry, University of Oregon, Eugene, Oregon 97403, United States

ABSTRACT: Macromolecular assembly at the interface between water and a hydrophobic surface underlies some of the most important biological and environmental processes on the planet. Important model systems for understanding this assembly at such interfaces are polyelectrolytes that have hydrophilic units interspersed along a hydrophobic polymer backbone, similar to many biological macromolecules. This feature article provides recent advances in the molecular factors that contribute to the adsorption and assembly of carboxylic acid-containing polyelectrolytes at the carbon tetrachloride−water interface, a model system for an oil−water interface. Using vibrational sum frequency spectroscopy and interfacial tension techniques, these unique set of studies presented herein identify the factors that dictate whether or not polyelectrolytes will adsorb to the oil−water interface and also describe the specifics of the adsorption process that depend upon factors such as polymer size, charge density, hydrophobicity, conformation, and the effect of metal ion electrostatics and bonding.

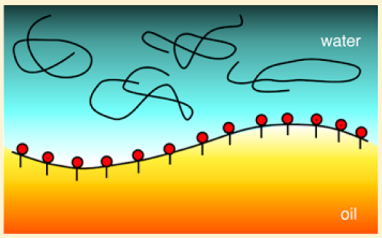

INTRODUCTION

Polyelectrolytes are a ubiquitous class of molecules that occur naturally in the form of proteins, DNA, enzymes, and humic acids and can also be synthesized to produce extensive libraries of polyelectrolytes that are used in a multitude of applications. Polyelectrolytes have particular relevance at the interface between two phases. The boundary between two immiscible fluids (i.e., a liquid−liquid interface and, most often, an oil−water interface) is an important locale for the adsorption and assembly of such charged macromolecules, having significance in biology, environmental remediation, and industry. For example, the behavior of charged biological macromolecules at fluid cell surfaces is important to several life functions.[1] The adsorption of charged environmental macromolecules to the interface between oil and water has importance in water remediation[2−5] and understanding the fate and transport of toxic materials.[6−9] In industrial applications, the assembly of polyelectrolytes at oil−water interfaces is essential to the stabilization of emulsions for a variety of processes[10−13] such as enhanced oil recovery, efficient drug delivery, and the manufacturing of personal care products. The behavior of polyelectrolytes at these fluid interfaces determines their degree of effectiveness in these important biological, environmental, and industrial processes.

It is especially important to understand (a) the specific conditions that favor or discourage polyelectrolyte surface adsorption; (b) interfacial adsorption dynamics under these various conditions; and (c) the resulting polyelectrolyte surface structures. As several polyelectrolytes consist of long hydrophobic backbones with charged hydrophilic functional groups equally spaced along the polymer chain, one might expect that the interfacial activity of a polyelectrolyte will depend upon a balance between hydrophobicity and hydrophilicity. Such a balance has been extensively studied in the behavior of alkyl chain surfactants at the oil−water interface, in which charging of the surfactant headgroup was found to be essential in its ordered interfacial assembly.[14] Compared to alkyl surfactants that consist of a single charged polar headgroup with a long hydrophobic tail, this balance has the potential to be very different for macromolecules with charges that persist along a hydrophobic chain. Understanding this balance on a molecular level is thus essential for describing less well understood fundamental processes that involve charged macromolecular assembly at the boundary between water and nonpolar fluids. A preliminary understanding of the adsorption of charged macromolecules to hydrophobic liquid−liquid interfaces has been achieved through interfacial tension measurements.[15−18] However, such measurements only give general information pertaining to polyelectrolyte adsorption dynamics and resulting interfacial structure and fail to give the molecular-level details necessary to fully characterize the behavior of polyelectrolytes at the oil−water interfaces.

Vibrational sum frequency (VSF) spectroscopy has proven to be a powerful technique to probe the molecular-level details of buried oil−water interfaces that are otherwise difficult to access.[19−29] This technique is well established,[30−34] and several excellent reviews exist on the subject.[35−39] A brief description is provided here as it pertains to the studies discussed in this article. In VSF spectroscopy, a fixed frequency visible beam and a tunable IR beam are overlapped at the oil−water interface. The generated sum frequency signal produces vibrational spectra of oriented interfacial molecules adsorbed to an oil−water interface and can give specific information regarding bond strengths, interactions between chemical species, and molecular orientations.[30,35,36] The interfacial selectivity stems from the fact that second-order nonlinear optical processes are

Received: July 8, 2014
Revised: September 23, 2014
Published: October 8, 2014

   dx.doi.org/10.1021/jp5068022 | J. Phys. Chem. C 2014, 118, 28331−28343

generally forbidden in centrosymmetric media, such as most bulk phases. At the interface between two such bulk phases, this symmetry is broken, causing the sum frequency process to selectively probe interfacial molecules. This symmetry rule also requires that the functional groups of interfacial molecules have a net orientation. By implementing different polarization combinations of the incident and detected beams, different orientational components of the interfacial molecules can be probed.

This technique has already been a useful tool for studying charged biological macromolecules at air–water,[39−46] solid–liquid,[39,41,44,45,47−54] and membrane interfaces,[39,44−46,55−60] including polyelectrolytes at the air–water[61−63] and solid–liquid[64−69] interfaces. While informative, these previous VSF studies do not capture the role of a unique oil–water interfacial environment on polyelectrolyte adsorption and assembly. For example, the majority of the solid–liquid studies focused on the adsorption of a polyelectrolyte onto an oppositely charged surface.[64−66,68,69] In this case, electrostatic interactions are found to dominate polyelectrolyte adsorption behavior, which is contrary to what is expected for its adsorption to a liquid–liquid interface. Despite the fluidity of the air–water interface, the vapor phase lacks the ability to specifically interact with the hydrophobic moieties of polyelectrolytes, as is the case for the nonpolar phase of an oil–water interface.

This article reviews the previous work performed in this laboratory of simple poly(carboxylic acids), specifically poly(acrylic acid) (PAA) and poly(methacrylic acid) (PMA), at the carbon tetrachloride–aqueous (CCl_4–H_2O) interface using VSF spectroscopy and interfacial tension studies. For the VSF studies presented here, the ssp polarization scheme (s-sum frequency, s-visible, p-IR) is employed to probe the functional groups of adsorbed polyelectrolytes that have orientational components that are normal to the interfacial plane. Specifically, spectra are obtained only of molecular components with a net orientation perpendicular to the oil–water interface. Poly(carboxylic acids), such as PAA and PMA, represent a class of polyelectrolytes that serve as good models for more complex environmental[70] and biological[71] macromolecules. Because their charging behavior, and thus their degree of hydrophobicity, is tunable, they also represent ideal systems with which to probe the competing effects of hydrophobicity vs hydrophilicity on the oil–water interfacial behavior. Here, studies of PAA and PMA as a function of both polyelectrolyte characteristics and solution conditions provide details concerning the molecular-level factors that dictate whether polyelectrolytes remain water solvated or adsorb to the oil–water interface, as well as the manner in which polyelectrolyte interfacial assembly specifically occurs. Interestingly, the conditions that influence the adsorption of these polymer surfactants are quite different than those that affect the oil–water interfacial behavior of well-studied alkyl surfactants.

Chemical structures of the polyelectrolytes discussed in this feature article are shown in Figure 1. Studies of PAA are first discussed, as PAA serves as a very simple model system. The results obtained from these studies have provided fundamental information pertaining to polyelectrolyte behavior at the oil–water interface. Studies of PMA, which serves as a more complex polyelectrolyte, are presented next. Our studies of PMA have allowed for examining the roles of increasing polyelectrolyte hydrophobicity and altering backbone properties by comparing the behavior of the different isomers of PMA, specifically isotactic PMA (iPMA) and syndiotactic PMA (sPMA), at the oil–water interface. The results presented show important molecular-level features of polyelectrolyte adsorption to the oil–water interface that persist throughout all systems examined, including the influence of polyelectrolyte charging on adsorption and desorption, the factors that affect the degree to which polyelectrolyte accumulates at the interface, and how interactions of polyelectrolytes with counterions can lead to induced adsorption. The article concludes with an overview of these features, how they compare to more well-understood alkyl chain surfactant systems, and future prospects for understanding more complex systems at the oil–water interface using VSF spectroscopy and interfacial tension measurements.

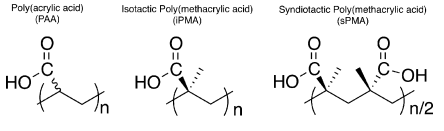

Figure 1. Chemical structure of the polyelectrolytes discussed in this work, specifically poly(acrylic acid) (PAA), isotactic poly(methacrylic acid) (iPMA), and syndiotactic poly(methacrylic acid) (sPMA).

POLY(ACRYLIC ACID): A SIMPLE MODEL POLYELECTROLYTE

Due to its simple repetitive carboxylic acid monomer unit, PAA serves as a good model system to study polyelectrolyte interfacial behavior using VSF spectroscopy. The balance between polyelectrolyte adsorption and solvation can easily be probed by influencing charge with the presence of a pH-sensitive carboxylic acid group. At low pH, most of the carboxylic acid groups are protonated and the polyelectrolyte is neutral. At high pH most of the carboxylic acid groups are deprotonated, and the polyelectrolyte is negatively charged. The pK_a of PAA (6–7) is higher than that of the corresponding acrylic acid monomer (4.5) due to the increasing difficulty to further remove protons as the charging increases on the polyelectrolyte.[72−74] The degree of polyelectrolyte charging changes PAA conformation in bulk solution. Specifically, PAA exists in a more coiled conformation at low pH when it is neutral and gradually extends its conformation as the pH increases and the polyelectrolyte becomes more charged, thus reducing charge–charge repulsive interactions.[75] The influence of polymer charging on the adsorbed surface structure of PAA can be examined spectroscopically by probing the modes of the carboxylic acid groups. Specifically, the presence of the carbonyl stretching mode near 1730 cm^{-1} signifies the presence of neutral, protonated carboxylic acids, while the presence of the carboxylate stretching mode near 1400 cm^{-1} signifies the presence of deprotonated, charged carboxylic acid groups.[76]

Initial VSF and surface tension studies of PAA by Beaman et al.[24] reveal the powerful role of charging in its adsorption to the oil–water interface. These results, shown in Figure 2, indicate very distinct and sharp pH dependence in the PAA adsorption. PAA (MW = 450 kDa) only adsorbs to the CCl_4–H_2O interface at pH ≤ 4 with negligible adsorption only a few tenths of a pH unit beyond pH 4. At the low pH values (Figure 2A, red data points), which correspond to a bulk polymer charge density of less than 20%, an intense peak appears near 1730 cm^{-1} in the VSF spectra and indicates a high degree of ordering of the protonated carboxylic acid functional groups of PAA. Spectra in the CH/OH stretching region also revealed a high degree of ordering of the polymer backbone methylene

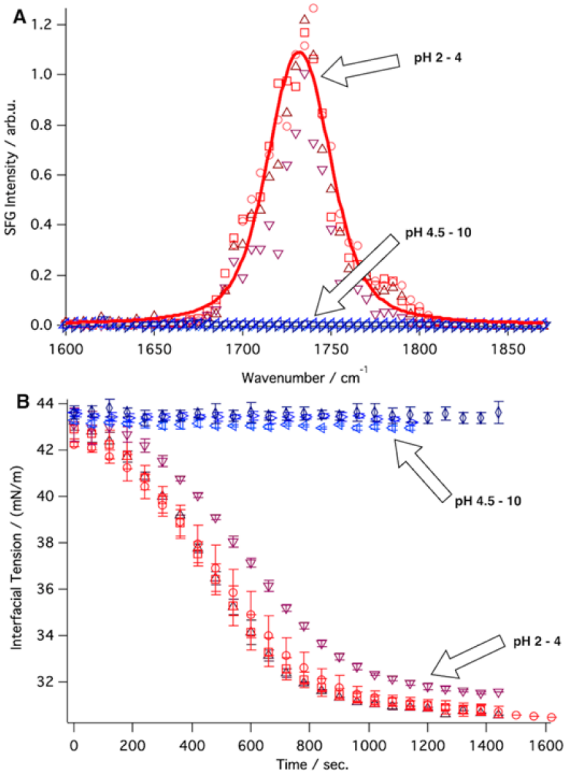

Figure 2. pH-dependent VSF spectra (A, ssp polarization) and interfacial tension measurements (B) of PAA (450 kDa, 5 ppm). Adapted with permission from ref 24. Copyright 2011 American Chemical Society.

groups.[24] This ordered extended interfacial conformation is in contrast to the random coil polymer conformation that is shown to exist in bulk solution for PAA at low pH values. The data also do not show dramatic changes in the carbonyl spectra from pH 1.5 to 4 (Figure 2A, red data points), and these spectra can be fit to the same single peak at 1730 cm^{-1} (Figure 2A, red trace). Additionally, there is no spectral evidence for the presence of oriented deprotonated carboxylate groups. The lack of signal in the carboxylate stretching region is attributed to VSF signal cancelation due to the carboxylate groups adopting opposite orientations to minimize unfavorable charge−charge repulsions.

At pH ≥ 4.5, the spectroscopic measurements in the carbonyl (Figure 2A, blue data points) and CH/OH[24] stretching regions reveal an interface completely devoid of polymer. The alternative explanation that polymer is present at the interface but so disordered as to not be measurable by VSF is discounted by the surface tension measurements that indicate no adsorption at pH ≥ 4.5. Despite the fact that PAA undergoes a gradual conformational transition with increasing the pH of the bulk solution, the VSF spectroscopic data show a sharp transition between PAA adsorption and desorption, with the adsorbed polyelectrolyte structure not significantly changing with changing pH. Such a sharp pH-dependent transition between complete polymer adsorption at pH 4 and desorption at pH 4.5 indicates the important nature of collective interactions between neighboring charges on the polymer chain.[77] Even though the charge density of PAA does not change much between pH 4 and 4.5, the accumulation of charges near each other on the polymer chain act to draw the PAA chains away from the interface and into the bulk water at pH 4.5 despite the fact that full coverage of the interface occurs at pH 4.

Interfacial tension measurements, shown in Figure 2B, reveal an intriguing aspect to the mechanism of PAA interfacial adsorption. As with the spectroscopic studies, these studies confirm that PAA adsorption occurs only at pH ≤ 4 (Figure 2B, red data points), with interfacial tension values dropping to ∼30 mN/m compared to the neat CCl_4−H_2O value of ∼45 mN/m.[78] At pH ≥ 4.5 (Figure 2B, blue data points), the interfacial tension does not change significantly compared to that of the neat CCl_4−H_2O interface, supporting that the lack of VSF signal at these pH values signifies an absence of polymer at the interface. Unlike the VSF spectroscopic studies, in which strong signal was observed within a minute of interface preparation (not shown), the interfacial tension took ∼10 min to reach an equilibrium value. The VSF signal only occurs from polymer functional groups that have a net orientation relative to the plane of the interface, while interfacial tension measurements are mainly sensitive to the relative amount of material at the interface. These results therefore show that PAA adsorbs to the interface in a multistep process. First, the VSF spectroscopic data indicate that polymer chains quickly adsorb to the interface and spread out with their backbone and protonated carboxylic acid functional groups having an average net orientation normal to the plane of the interface. This conformation is very different from that shown to exist in the bulk at these low pH values. Such a rapid process is in part attributed to the inherent oil−water interfacial field, which is known to assist in the adsorption of charged species.[27,79] PAA adsorption to the interface over time is disordered and so is revealed only by the interfacial tension data. Subsequent polymer adsorbs due to favorable hydrophobic interactions with the initially adsorbed layer but is not ordered because the field is likely unable to penetrate far enough into the bulk to cause the ordering of this second layer.[24]

The interfacial tension measurements at pH 2 of PAA of varying molecular weight[23] and concentration,[22] shown in Figure 3, further confirm this multistep adsorption process. In the VSF spectroscopic studies of 1.8, 450, and 1250 kDa PAA, a strong signal was again seen in the CH and carbonyl stretching regions within a minute after interface preparation,[23] indicating the rapid adsorption of highly ordered polymer layers. The VSF spectra of the carbonyl peaks were the same within error for all molecular weights, indicating a very similar surface structure among polymer sizes. The corresponding interfacial tension data, shown in Figure 3A, indicate that the smallest PAA polymer (1.8 kDa) takes only minutes to reach an equilibrium value of ∼30 mN/m, while the largest PAA polymer (1250 kDa) takes hours to stabilize near this value. Despite the difference in the adsorption kinetics of the disordered polymer layers, the amount of PAA adsorbed at equilibrium is relatively the same for all polymer sizes.

Concentration studies of 450 kDa PAA also display time-dependent behavior in the adsorption of the disordered polymer layer. VSF spectra in the CH/OH and carbonyl stretching regions for polymer concentrations from 1 to 50 ppm again showed the rapid adsorption of a highly ordered interfacial layer structure that did not significantly change with concentration.[22] Interfacial tension measurements, shown in Figure 3B, reveal that the time for the disordered polymer to adsorb to the interface is longer for the lower concentration samples. Both the molecular weight and concentration studies support the multistep adsorption process, showing that the

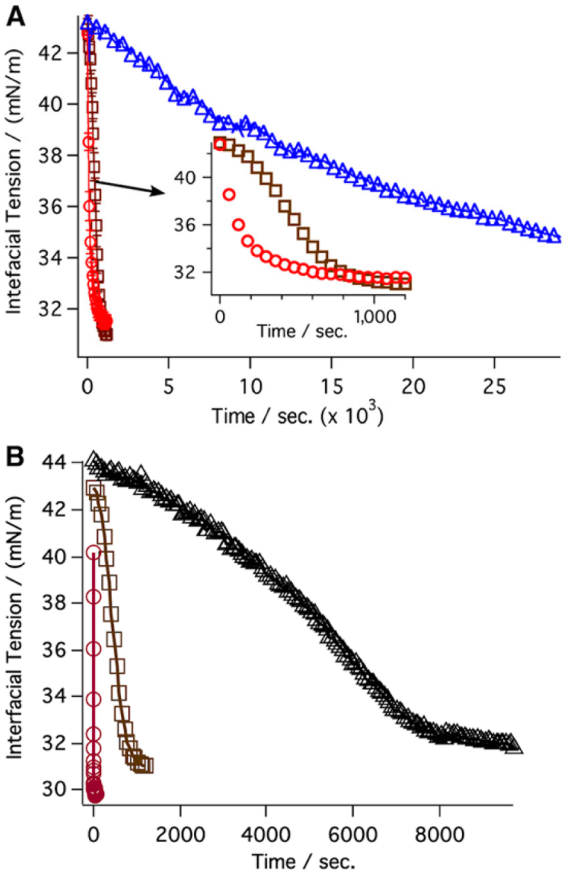

Figure 3. Time-dependent interfacial tension measurements of PAA (pH 2) as a function of (A) molecular weight (1.8 kDa, red circles; 450 kDa, brown squares; 1250 kDa, blue triangles) and (B) concentration (50 ppm, maroon circles; 5 ppm, brown squares; 2 ppm, black triangles). Data are taken from refs 22 and 23.

initial rapid adsorption step is strongly dictated by the interfacial field, while the second slower adsorption step is dictated by the diffusion of disordered polymer to the interface. Figure 4 depicts this pH-dependent multilayer adsorption process. The combination of results from the VSF spectroscopic and interfacial tension techniques provides a more complete picture for polyelectrolyte interfacial behavior that would otherwise not be obtained with just one technique or the other.

While the molecular weight and concentration studies of PAA at a low pH provide a clear picture for multistep polymer adsorption, the studies do not address the aspect of the balance between polymer charging and hydrophobicity. Charging of the polymer drives the polymer into the aqueous phase, and hydrophobicity drives the polymer to the interface, which is expected in macromolecular oil–water interfacial adsorption and assembly. Our studies have revealed that when PAA is neutral the overall equilibrium structure of the initially adsorbed PAA layer and the total amount of disordered PAA adsorbed are relatively the same despite differences in either polymer size or concentration, which has been observed in other polymer systems.[80,81] In order to further probe the role of charging in polyelectrolyte interfacial behavior, PAA was studied in the presence of different salts. These VSF spectroscopic and interfacial tension results, shown in Figure 5, reveal that both divalent and monovalent cations are able to induce the ordered adsorption of 450 kDa PAA to the oil–

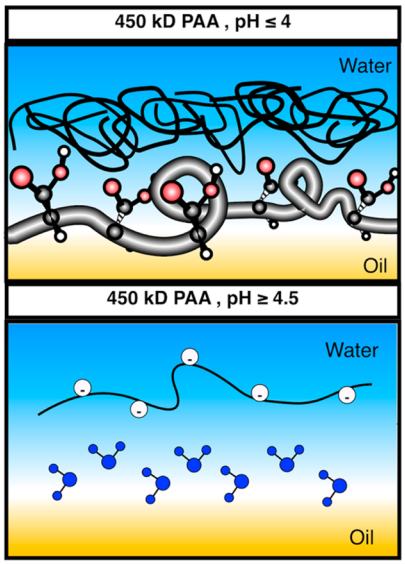

Figure 4. Cartoon depicting the pH-dependent adsorption behavior of PAA (450 kDa, 5 ppm) at the oil–water interface. At pH ≤ 4 (top) PAA adsorbs to the interface as multilayers, while at pH ≥ 4.5 (bottom), PAA remains water solvated.

water interface at pH values when it is not normally surface active, albeit to different degrees.[22]

As shown in Figure 5A, Ca^{2+} induces the adsorption of 450 kDa PAA to the interface at pH 4.5, causing both the carbonyl and carboxylate groups to adopt a net orientation normal to the interfacial plane. As seen with PAA at low pH, the VSF signal was seen almost instantaneously and did not significantly change with time. Therefore, the decrease in interfacial tension over time, as seen in Figure 5B, again indicates the multilayer adsorption process. PAA with Mg^{2+} had a similar VSF spectroscopic response, yet the signal intensities in both the carboxylate and carbonyl stretching regions were weaker than PAA with Ca^{2+}.[22] Because the interfacial tension data, and thus relative amount of adsorbed disordered polymer, were the same within error for PAA with Ca^{2+} and Mg^{2+}, the difference in sum frequency signal intensity indicates that the carboxylic acid and carboxylate groups of the initially adsorbed PAA layer are more ordered with Ca^{2+} compared to Mg^{2+}. This is attributed to the weaker induced field strength of solvated Mg^{2+} ions compared to solvated Ca^{2+} ions, as has been shown previously from molecular orbital calculations.[82] The appearance of the deprotonated carboxylate peak is consistent with a mechanism for cation-induced PAA adsorption at higher pH values in which the positively charged divalent cations screen the negatively charged carboxylate groups. The charge screening additionally allows for the ordering of the carboxylate groups at the interface, which is not apparent with PAA at lower pH values.

The addition of Na^{+} to 450 kDa PAA at pH 4.5 also induces polyelectrolyte adsorption; however, there are differences in the data compared to that of PAA with divalent cations. Specifically, as seen in the VSF spectroscopic data in Figure 5C, the ordering of the protonated carboxylic acid groups is observed by the strong peak in the carbonyl stretching region. The lack of ordering of the carboxylate groups is observed by the absence of signal in the carboxylate stretching region. Additionally, the lack of significant adsorption of disordered polymer to the interface over time is observed by the small

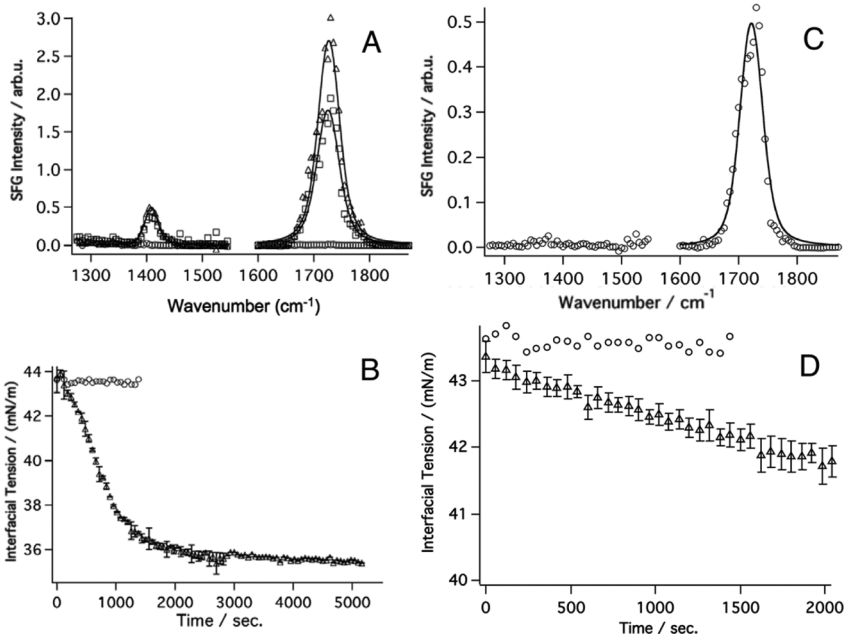

Figure 5. VSF spectra (top, ssp polarization) and interfacial tension measurements (bottom) of 450 kDa PAA (5 ppm, pH 4.5) with added ions. (A) PAA in the absence of added ions (circles), with 0.5 mM $CaCl_2$ (squares) and 1 mM $CaCl_2$ (triangles). (B) PAA in the absence of ions (circles) and with 1 mM $CaCl_2$ (triangles). (C) PAA with 3 mM NaCl. (D) PAA in the absence of ions (circles) and with 3 mM NaCl (triangles). Data are taken from ref 22.

change in the measured interfacial tension relative to that of the neat CCl_4–H_2O interface, as shown in Figure 5D. It is well established that monovalent cations interact less effectively with polyanions compared to divalent cations. Specifically, on average monovalent cations are only able to penetrate the first solvation shell of polyanions, while divalent cations are better able to penetrate the second solvation shell of polyanions.[83,84] Due to these weaker interactions of monovalent cations with partially solvated polyanions, Na^+ is able to induce the adsorption of PAA to the interface, but it is unable to effectively screen the negative charges of the polymer chain to cause the net orientation of the charged carboxylate groups of the initially adsorbed layer. The lack of charge screening at the interface additionally hinders favorable hydrophobic interactions between the initially adsorbed PAA layer and the PAA in bulk solution so that the adsorption of disordered layers to the interface over time does not occur. These results support the picture of induced PAA adsorption through the screening of negatively charged carboxylate groups by positively charged ions and that the degree of interfacial adsorption and ordering depends upon the degree that the cation effectively screens the polymer charges. Figure 6 shows a cartoon depicting the difference in Ca^{2+} vs Na^+ PAA induced adsorption.

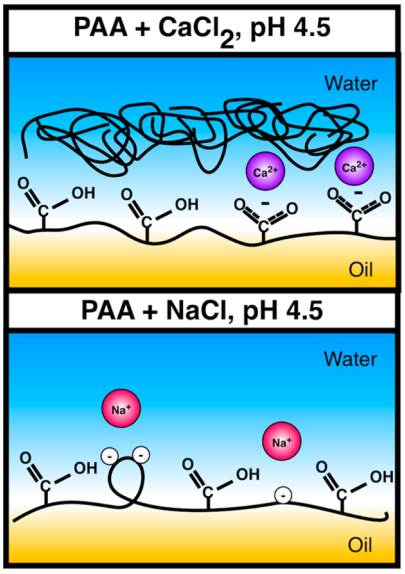

Figure 6. Cartoon depicting the induced adsorption of PAA at pH 4.5 with $CaCl_2$ (top) and NaCl (bottom).

POLY(METHACRYLIC ACID): INCREASING POLYELECTROLYTE COMPLEXITY

The studies of PAA provide fundamental information concerning the molecular-level details of the oil–water interfacial behavior of a very simple polyelectrolyte. In order to understand a more complex polyelectrolyte, VSF spectroscopic and interfacial tension studies were conducted of poly(methacrylic acid) (PMA). Compared to PAA, PMA is overall more hydrophobic due to the presence of methyl groups on the polymer chains. Different chiral isomers of PMA are available that have very different bulk properties. These isomers are shown in Figure 1. For the syndiotactic PMA (sPMA), the chirality alternates between monomers, while for the isotactic PMA (iPMA), all monomers have the same chirality. In bulk solution, it has been shown the iPMA is overall more hydrophobic than sPMA.[85−88] Additionally, the close proximity of the carboxylic acid groups relative to each other for iPMA provides it with a higher charge density than for sPMA in bulk solution.[86−88] The studies of PMA discussed below show how this different bulk behavior manifests at the oil–water interface and also displays the important facets of polyelectrolyte adsorption seen in the studies of PAA.

VSF spectroscopic and interfacial tension measurements of 3 kDa sPMA as a function of pH, as shown in Figure 7, reveal that its adsorption behavior is very similar to that of 450 kDa

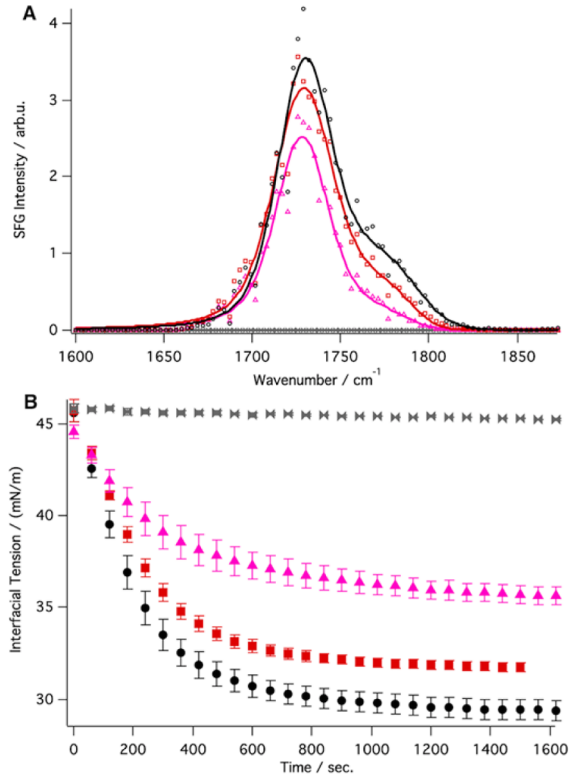

Figure 7. VSF spectra (A, ssp polarization) and interfacial tension measurements (B) of 3 kDa sPMA (5 ppm) at varying pH values (pH 5.5, gray bowties; pH 5, pink triangles; pH 4, red squares; pH 2, black circles). Data are taken from ref 28.

PAA, albeit with some differences.[28] As shown in Figure 7A, the peaks due to the carbonyl stretching mode appear only at relatively low pH values, specifically at pH $\leq$ 5. At pH $\geq$ 5.5, the VSF signal does not appear in the carbonyl stretching region, and the CH/OH stretching region spectra confirm a lack of polymer adsorption to the oil–water interface at these higher pH values.[28] Unlike PAA, however, two features appear in the spectra: a lower frequency peak near 1730 cm^{-1} that corresponds to carbonyl groups in a more water-rich environment[76] and a higher frequency peak near 1790 cm^{-1} that corresponds to carbonyl groups in a more oil-rich environment.[89] The presence of the higher frequency peak in Figure 2A, which does not appear in the PAA spectra, suggests that sPMA sits further into the oil phase than PAA due to the higher degree of hydrophobicity for PMA compared to PAA. As the pH is decreased from 5 to 2, the spectra in Figure 7A show an increase in the intensities of both the water-rich and oil-rich carbonyl peaks. This indicates that as the pH decreases and the charged carboxylate groups become protonated there is an increase in the number of oriented carbonyl groups pointing into both the water and oil phases.

The degree of charging of the quick adsorbing and ordered sPMA layer plays a large role in the degree to which disordered polymer accumulates at the interface over time. Like PAA, the VSF signal seen from the sPMA appeared within a minute of interface preparation and did not appear to change with time. The time dependence seen in the interfacial tension data of sPMA, shown in Figure 7B, therefore indicates that, like PAA, sPMA adsorbs in a multistep process. At pH 5.5, the interfacial tension value of sPMA does not change relative to that of the neat CCl_4–H_2O interface (45 mN/m), confirming the absence of polymer at the interface. As the pH decreases from 5 to 2, a decrease in the equilibrium interfacial tension value is observed. This indicates that a decrease in the degree of charge–charge repulsive interactions between polymer layers leads to an increase in the amount of disordered polymer that is able to accumulate at the oil–water interface. This pH-dependent behavior is consistent with the conclusion that hydrophobic interactions between the initially adsorbed, ordered layer and the remaining disordered polymer in bulk solution are key in the multistep adsorption process.

The pH-dependent interfacial behavior of 3 kDa sPMA (~34 monomers per chain) is slightly different than that of 450 kDa PAA (~6250 monomers per chain). Specifically, there is a more gradual pH transition between adsorption and desorption in the sPMA data compared to the sharp pH transition between adsorption and desorption observed in the PAA data. It is likely that the more hydrophobic nature of PMA allows it to more readily adsorb to the oil–water interface at higher pH values compared to PAA. However, the slight differences in pH-dependent adsorption may not be entirely due to the differences in the chemical structures of the different polymers but also may in part be due to the number of monomers comprising the polymer chains. This is supported by VSF spectroscopic and interfacial tension studies of 28 kDa sPMA (326 monomers per chain) as a function of pH, shown in Figure 8.

Here, the spectroscopic data in the carbonyl stretching region of the 28 kDa sPMA in Figure 8A are very similar to that of the 3 kDa sPMA in Figure 7A, but only at pH $\leq$ 4, with an increase in peak intensity seen for both the water-rich and oil-

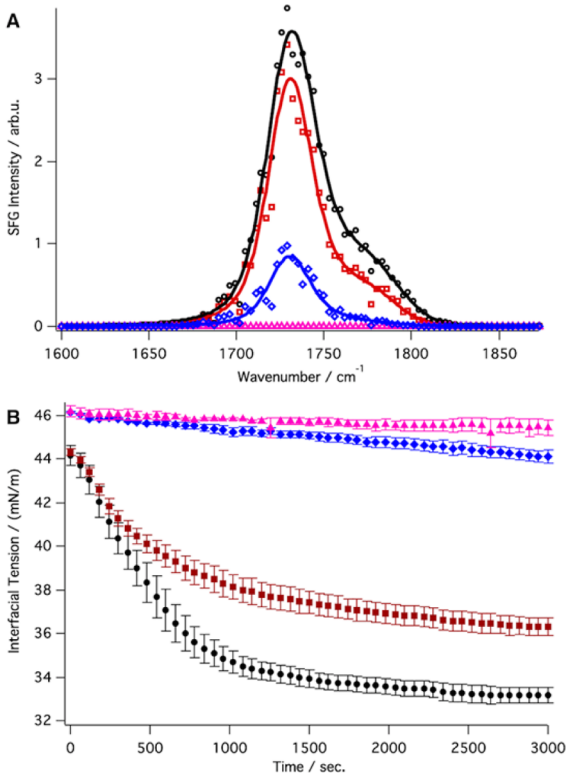

Figure 8. VSF spectra (A, ssp polarization) and interfacial tension measurements (B) of 28 kDa sPMA (5 ppm) at different pH values (pH 5, pink triangles; pH 4.5, blue diamonds; pH 4, red squares; pH 2, black circles). Data are taken from ref 28.

rich carbonyl features with decreasing pH. The time dependence seen in the interfacial tension data at these lower pH values, shown in Figure 8B, additionally indicates a multistep adsorption process. Key differences in the data occur at pH > 4. Specifically, adsorption does not begin until pH 5 for the 28 kDa polymer, as seen by the lack of VSF signal in the carbonyl stretching region (Figure 8A) as well as a lack of lowering of the interfacial tension relative to the neat oil–water interface (Figure 8B). Additionally, the structure of the 28 kDa sPMA that adsorbs to the interface between pH 4 and 5 is very different from that of the 3 kDa sPMA in the same pH region. In the carbonyl stretching region, a very weak water solvated feature indicated by its low energy dominates the spectrum. The interfacial tension data show only a very small decrease over time, indicating an absence of the multistep adsorption process.

Importantly, unlike the 28 kDa sPMA at lower pH values, time dependence is observed in the VSF signal intensity between pH 4 and 5.[28] Here, there is an initial increase in the CH and carbonyl sum frequency signal intensity followed by a decrease and eventual stabilization. The carbonyl spectrum of 28 kDa sPMA at pH ∼ 4.5 shown in Figure 8A was taken after this signal had stabilized. The continual decrease in the interfacial tension value with time for this sample indicates that the decrease in VSF signal intensity is consistent with polymer reorientation rather than desorption. Additionally, the spectrum of 28 kDa sPMA at pH ∼ 4.5 in the water OH stretching region shows the presence of oriented water molecules that straddle the oil–water interface, indicating incomplete coverage of the interface by the polymer.[28] These data suggest that only a thin layer of the 28 kDa sPMA adsorbs to the oil–water interface, with reorientation of polymer chain segments protruding into the bulk water occurring after a critical amount of polymer has adsorbed in order to minimize charge–charge repulsions.

Investigations of the interfacial behavior of different size sPMA chains support the presence of collective charging behavior seen in PAA that induces its sharp pH-dependent adsorption behavior. For the 3 kDa sPMA, only a few charges can accumulate per chain as the pH increases, while for the 28 kDa sPMA, many more charges can accumulate per chain as the pH increases. Due to cooperative interactions, these charges accumulate near each other on the polymer chains, causing the smaller polymer to be much more surface active at higher pH values compared to the larger polymer. Between pH 4 and 5, the highly charged segments of the 28 kDa sPMA chain are drawn away from the interface and into the bulk water, as depicted in Figure 9. For the 450 kDa PAA, the large number of charges that can accumulate per chain likely contributes to its very sharp pH-dependent adsorption behavior.

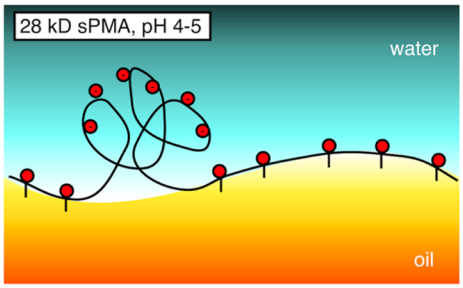

Figure 9. Cartoon depicting the oil–water interfacial behavior of 28 kDa sPMA at pH 4–5.

A key feature observed in the PAA and sPMA adsorption to the oil–water interface at low pH is the ability to form multilayers from favorable hydrophobic interactions between the quickly adsorbing ordered layer and the disordered polymer that accumulates to the interface over time. The VSF spectroscopic and interfacial tension measurements at pH 2 comparing sPMA to iPMA in Figure 10, however, show that

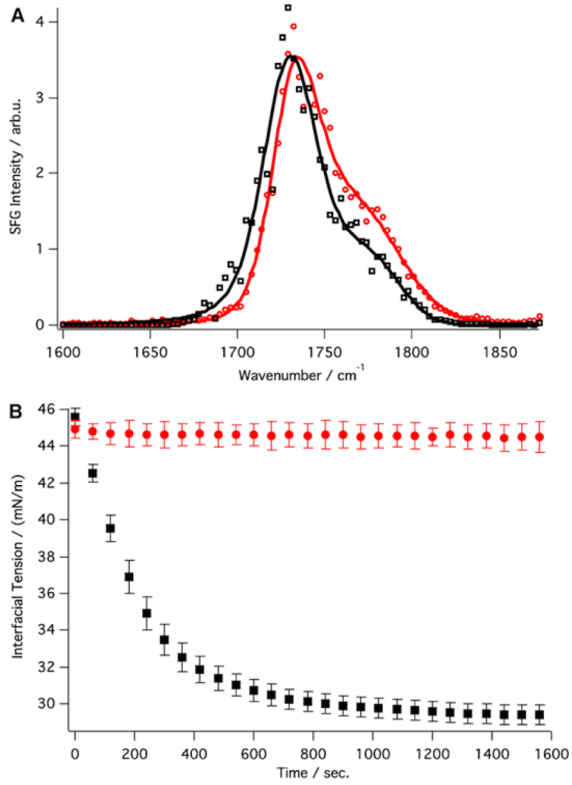

Figure 10. VSF spectra (A) and time-dependent interfacial tension measurements (B) for 3 kDa sPMA (black squares) and iPMA (red circles) at pH 2.

this property is not inherent in all polyelectrolytes and strongly depends on the adsorbed polyelectrolyte conformation.[23,90] As discussed previously, iPMA has the same chemical composition as sPMA, yet has a different backbone configuration (Figure 1). This difference is shown to lead to different adsorbed polymer structures at the oil–water interface.[23,90] The strong signal present in the VSF spectra in the carbonyl stretching region, as shown in Figure 10A, indicates that both iPMA and sPMA adsorb to the interface with a net orientation of the carbonyl groups normal to the interfacial plane. The spectra are very similar for the different isomers, containing both the water-rich and oil-rich carbonyl features. The oil-rich feature for iPMA, however, is slightly more intense than for sPMA, suggesting that iPMA sits further into the oil phase than sPMA. This is not surprising, as iPMA is known to be overall more hydrophobic than sPMA.

Despite the similarity in the carbonyl region spectra, the interfacial tension measurements are drastically different for the two isomers, as shown in Figure 10B. Here, the interfacial tension of the sPMA sample decreases over ∼10 min until an equilibrium value of ∼30 mN/m is reached, while the interfacial tension of iPMA does not change very much over time compared to the neat CCl_4–H_2O interfacial tension value of 45 mN/m.[23] The VSF spectroscopic results indicate that, like

sPMA and PAA, iPMA quickly adsorbs to the interface as a highly ordered polymer layer. Unlike sPMA and PAA, however, the interfacial tension measurements reveal that disordered polymer does not continue to accumulate at the interface over time. Spectra in the CH/OH stretching region,[23,28,29] as well as preliminary computational results,[90] indicate that the conformations of the initially adsorbed iPMA and sPMA polymer layers are quite different. Specifically, the hydrophobic residues of iPMA mainly reside in the oil phase, while those of sPMA have the ability to reside in the water phase. This allows for favorable hydrophobic interaction to exist between the initially adsorbed sPMA and the polymer that remains in bulk solution, yet these interactions are hindered for iPMA. Figure 11 depicts the multilayer adsorption of sPMA compared to the single-layer adsorption of iPMA.

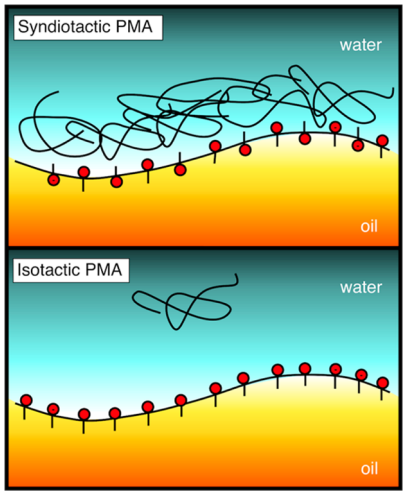

Figure 11. Cartoon depicting the multilayer adsorption process for sPMA (top) and monolayer adsorption process for iPMA (bottom).

Polyelectrolyte backbone configuration not only plays a role in whether or not multilayer formation occurs but also affects the degree to which counterions screen the negatively charged carboxylate groups and induce polyelectrolyte adsorption to the oil–water interface. Specifically, like PAA, both monovalent and divalent cations induce the adsorption of iPMA to the interface at high pH values, yet this is not the case with sPMA.[29] That iPMA can adsorb to the interface in the presence of ions but that sPMA cannot is attributed to the fact that the configuration of iPMA gives it an extremely high charge density allowing it to interact more strongly with oppositely charged species in bulk solution compared to sPMA.[86−88] Unlike PAA that adsorbs to the interface at high pH values in the presence of monovalent and divalent cations, the placement of the methyl groups on sPMA acts to sterically hinder interactions of the carboxylate groups with the counterions such that charge screening does not occur to an extent that favors sPMA adsorption. For iPMA, the strong interactions with counterions, particularly with Ca^{2+}, lead to an induced adsorption process that is quite complex.

VSF spectroscopic measurements of iPMA with $CaCl_2$ in the CH/OH stretching region, shown in Figure 12, indicate that Ca^{2+} ions induced the adsorption of iPMA to the interface at a solution pH not conducive to polymer adsorption. In the absence of added salt, the spectrum of iPMA at pH 6 does not reveal ordered polymer at the interface. Specifically, the spectrum looks very similar to that of the neat CCl_4–H_2O interface, with the sharp peak near 3700 cm^{-1} corresponding to the "free OH" mode of water molecules that straddle the oil–water interface. As $CaCl_2$ is added to solution, CH peaks appear in the spectrum between 2800 and 3000 cm^{-1} and increase in intensity until an ionic strength of 0.5 mM $CaCl_2$, while the "free OH" mode disappears. At higher ionic strengths, however, the intensity of the CH peaks begins to decrease. Interfacial tension measurements, which neither showed dependence in $CaCl_2$ ionic strength nor showed that the added ions induced multilayer formation, indicated that the decrease in CH peak intensity with excess $CaCl_2$ was due to a reorientation of the polymer structure at the interface.[29,78]

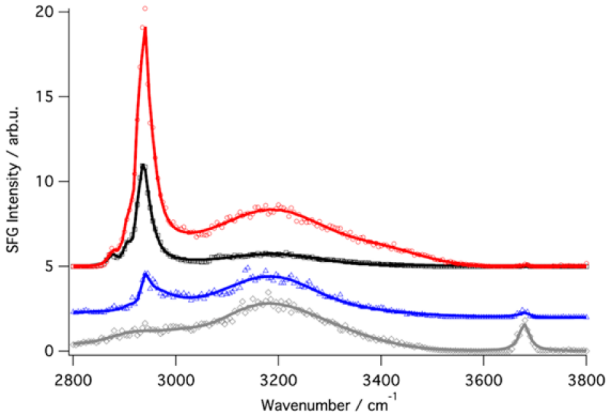

Figure 12. VSF spectra (ssp polarization) of 3 kDa iPMA (5 ppm, pH 6) as a function of $CaCl_2$ ionic strength (0 mM, gray diamonds; 0.1 mM, blue triangles; 0.5 mM, red circles; 10 mM, black squares). The data are offset for clarity. The solid lines are fits to the data. Data are taken from ref 29.

In order to further probe this reorientation process, and also to explore the interactions of the Ca^{2+} ions with the negatively charged carboxylate groups, spectra of the carboxylate and carbonyl regions of iPMA were also obtained as a function of $CaCl_2$ ionic strength.[29] The intensities of the methylene peak near 2930 cm^{-1}, the carboxylate peak near 1400 cm^{-1}, and the carbonyl peak near 1712 cm^{-1} are plotted in Figure 13. Unlike the methylene peak intensity, the carboxylate peak intensity increases until an ionic strength of 1 mM and then stabilizes at higher ionic strengths. The intensity of the carbonyl peak increases until a $CaCl_2$ ionic strength of 0.25 mM and then decreases in intensity with further increases in ionic strength. The intensity trends of the methylene, carboxylate, and carbonyl peaks with increasing $CaCl_2$ ionic strength do not match each other. This is not surprising, however, because Ca^{2+} is known to induce the deprotonation of poly(carboxylic acids).[91] Therefore, an increase in $CaCl_2$ ionic strength can lead to a decrease in the number of protonated carboxylic acid groups and thus increase the number of deprotonated carboxylate groups at the interface. When the peak intensities of the carboxylate and carbonyl peaks are considered together in Figure 13, showing the change in the relative number of both ordered carboxylate and carbonyl groups at the oil–water interface with increasing $CaCl_2$ ionic strength, the trend in the data follows that of the methylene peak intensity.

These data are consistent with the detailed picture of Ca^{2+}-induced adsorption of iPMA to the oil–water interface that is depicted in the bottom of Figure 13. Here, the initial addition of Ca^{2+} screens the charges of iPMA, making the polymer more hydrophobic and therefore driving it to the interface. Upon

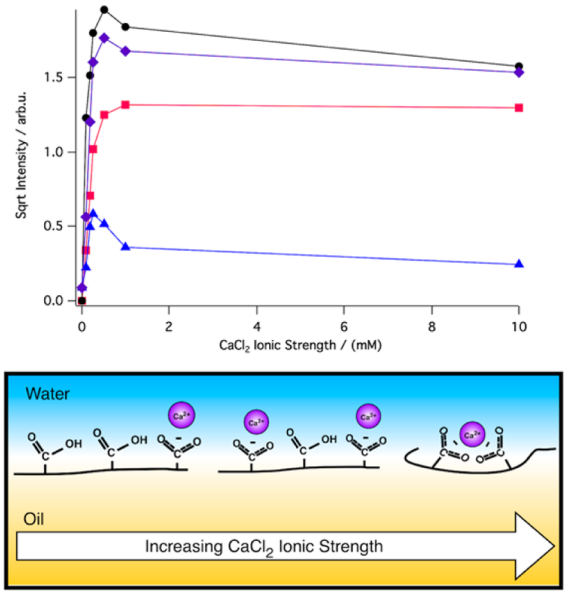

Figure 13. (Top) Square root of the peak intensities from the spectra of 3 kDa iPMA (5 ppm, pH 6) in the CH (2930 cm^{-1}, black circles), carboxylate (1400 cm^{-1}, pink squares), carbonyl (1712 cm^{-1}, blue triangles), and carboxylate + carbonyl (purple diamonds) stretching regions as a function $CaCl_2$ ionic strength. (Bottom) Cartoon depicting interfacial behavior of 3 kDa iPMA (5 ppm, pH 6) with increasing $CaCl_2$ ionic strength. Data are taken from ref 29.

increasing the ionic strength, the Ca^{2+} ions are able to induce the deprotonation of the carboxylic acid groups. At high enough ionic strengths, there is a reorientation of the interfacial polymer structure. This is likely due to the interaction of one Ca^{2+} ion with two neighboring carboxylate groups[84,92−95] that either increases the disorder of the adsorbed polymer or creates centrosymmetric structures that are not VSF active.

Interestingly, the signal intensity from iPMA with added $CaCl_2$, as shown in Figure 12, does not appear immediately. Rather, the signal intensity increases over time before stabilizing after several hours. The time for signal stabilization to occur increases with increasing $CaCl_2$ ionic strength, as shown in Figure 14. Here, at ionic strengths of 0.5 mM and below, the time for the signal to stabilize is on the order of a few hours, while for higher concentrations the signal takes over 12 h to stabilize. This long time dependence is in part attributed to adsorption of highly disordered, coiled chain structures[92,93,96−99] to the interface that subsequently spread at the interface due to favorable interactions between the polymer hydrophilic groups and the water and the hydrophobic groups with the oil. As clarified by previous bulk studies, these coiled chain structures increase in stability with increasing the number of interactions between the Ca^{2+} ions and the carboxylate groups,[95] and so the time for spreading increases with $CaCl_2$ ionic strength. The bottom of Figure 14 displays this multistep adsorption process.

As with PAA, monovalent cations are also shown to induce the adsorption of iPMA to the oil−water interface, and the interactions with the carboxylate groups are also found to be weaker than with divalent cations.[29] This is seen in the VSF spectra of iPMA with 10 mM ionic strength KCl compared to with 10 mM ionic strength $CaCl_2$, as shown in Figure 15. Here, the carbonyl peak near 1712 cm^{-1} for iPMA with K^+ is much more intense than for iPMA with Ca^{2+}, as shown in Figure 15A, while the carboxylate peak near 1400 cm^{-1} is much less intense

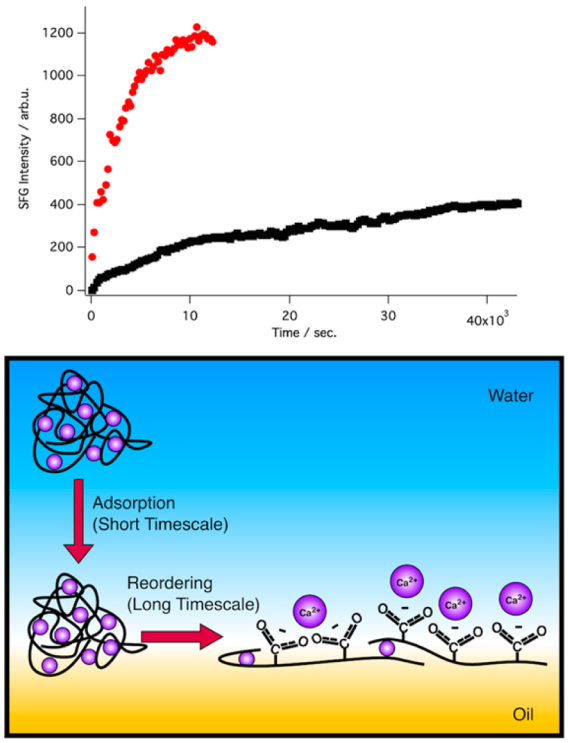

Figure 14. Time-dependent sum frequency signal intensity of the CH peak (ssp polarization) observed in the spectra of 3 kDa iPMA (5 ppm, pH 6) with 0.5 mM (red) and 10 mM (black) $CaCl_2$ (top). Cartoon depicting the multistep adsorption process for iPMA with Ca^{2+} at pH 6 (bottom). Data are taken from ref 29.

for iPMA with K^+ than for iPMA with Ca^{2+}, as shown in Figure 15B. This demonstrates the weaker interactions of the carboxylate groups with K^+ compared to Ca^{2+}. Specifically, the K^+ ions are not as well able to induce the deprotonation of the carboxylic acid groups as the Ca^{2+} ions, resulting in the relatively strong carbonyl peak intensity. Even though the electrostatic interactions of the K^+ ions with carboxylate groups decrease the overall polymer charge density and thus drive iPMA to the oil−water interface, these interactions are not strong enough to cause a high degree of ordering of the carboxylate groups, resulting in relatively weak carboxylate signal. This structure is consistent with that of interfacial PAA with Na^+, as shown in Figure 6.

POLYELECTROLYTES AS SURFACTANTS: AN OVERVIEW AND FUTURE PROSPECTS

The assembly of polyelectrolytes to the interface between nonpolar and aqueous liquids is an important process to several applications ranging from biological, to environmental, to industrial. It is therefore important to identify and understand which polyelectrolyte characteristics as well as aqueous solution conditions enable charged macromolecules to adsorb to liquid−liquid interfaces. Additionally, it is critical to acquire specific details of the adsorption process itself, as well as the resulting interfacial structure. Specific questions can be asked in terms of polyelectrolyte behavior at the oil−water interface: What characteristics of the polyelectrolyte and aqueous solution promote the ordered assembly of polyelectrolytes at the interface? What factors determine the degree to which polyelectrolytes accumulate at the interface? How can the interactions of polyelectrolytes with counterions induce

dx.doi.org/10.1021/jp5060932 | J. Phys. Chem. C 2014, 118, 28321−28342

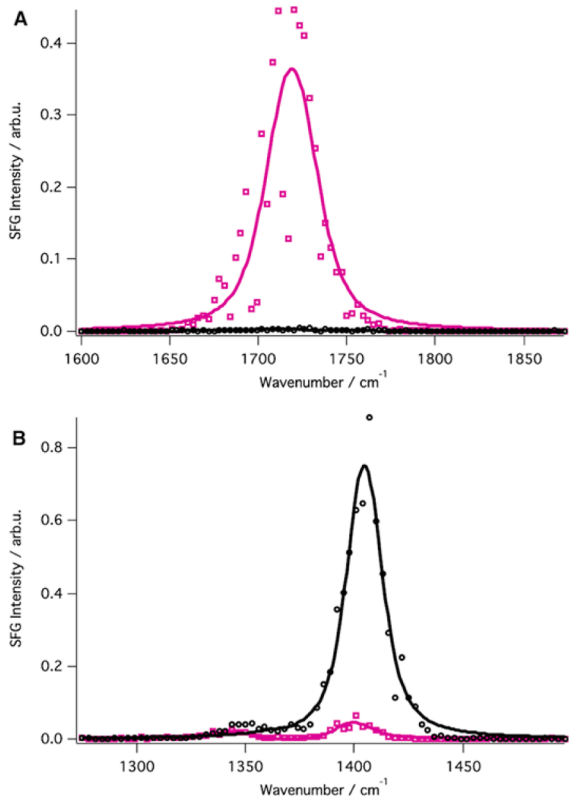

Figure 15. VSF spectra (ssp polarization) of 3 kDa iPMA (5 ppm, pH 6) with added 10 mM KCl (pink squares) and 10 mM $CaCl_2$ (black circles) in the carbonyl (A) and carboxylate (B) stretching regions. Solid lines are fits to the data. Data are taken from ref 29.

adsorption and affect polyelectrolyte adsorption dynamics and resulting interfacial structure? The combined VSF spectroscopic and interfacial tension studies performed in our laboratory have served to provide a fundamental molecular level understanding concerning polyelectrolyte adsorption and assembly at an oil–water interface, which has not been thoroughly studied previously. Several important features related to the balance between polyelectrolyte hydrophobicity and hydrophilicity have been discovered that greatly influence polyelectrolyte interfacial behavior and appear to be consistent throughout our studies of different poly(carboxylic acids).

Interestingly, these features of polyelectrolyte adsorption to the oil–water interface are somewhat different from those of simple, carboxylic acid-containing alkyl surfactants. For instance, alkyl surfactants adsorb to the oil–water interface in an ordered manner only at relatively high pH when most of the carboxylic acid groups are deprotonated, while polyelectrolytes adsorb to the oil–water interface in an ordered manner only at relatively low pH when most of the carboxylic acid groups are protonated. This indicates the powerful role of collective charging behavior in the oil–water interfacial assembly of a macromolecule that is able to accumulate several charges, compared to one that has only one ionizable group. Additionally, polyelectrolytes have the ability to adsorb either as a monolayer or as multilayers, depending on the conformation of the initially adsorbed polymer layer. This is in contrast to simple alkyl surfactants, which tend to quickly adsorb to the oil–water interface as a monolayer and lack the dynamics seen in polyelectrolyte adsorption. Lastly, cations have similar effects on the assembly of polyelectrolytes and alkyl surfactants at the oil–water interface at high pH values. For polyelectrolytes, cations can induce the adsorption of certain polyelectrolytes, with the degree of adsorption and ordering depending on the strength of the interaction between the carboxylate groups and the cations. Even though alkyl surfactants do adsorb to the interface at these higher pH values, the addition of cations induces an increased degree of packing and ordering on the surfactant monolayer, which also depends on the degree of the interaction of the cation with the carboxylate group.

The results presented in this article have thus provided an in-depth molecular-level picture for describing polyelectrolyte behavior at the oil–water interface. In particular, these results have implications for a variety of fields in which polyelectrolyte assembly between two immiscible liquids is important, such as for describing the behavior of proteins at the surface of a cell, understanding the fate and transport of toxins and nutrients in the environment via humic acids, or determining the ability of polyelectrolytes to stabilize emulsions for enhanced oil recovery. Often, polyelectrolytes are used with oppositely charged organic species, such as surfactants or other polyelectrolytes, to invoke synergistic adsorption effects. This is especially true for applications that require a significant lowering of the oil–water interfacial tension. We now have a thorough molecular-level understanding of both polyelectrolyte and alkyl surfactant behavior at the oil–water interface. However, these adsorption processes for mixed systems are complicated and not yet well understood. The studies presented here, as well as our previous studies of alkyl surfactants, have paved the way for future studies aimed at exploring these more complex polyelectrolyte-*co*-adsorbate systems at the oil–water interface with VSF spectroscopy that have prevalence in more realistic systems.

AUTHOR INFORMATION

Corresponding Author

* E-mail: richmond@uoregon.edu. Fax: 541-346-3422. Phone: 541-346-0116.

Notes

The authors declare no competing financial interest.

Biographies

Ellen J. Robertson received her B.A. in chemistry from Kalamazoo College in 2008 and her Ph.D. in chemistry from the University of Oregon in 2014. She currently holds a postdoctoral appointment at Lawrence Berkeley National Laboratory in Ronald Zuckermann's group where she studies the formation of peptoid nanosheets at an oil–water interface.

Geraldine L. Richmond is the Presidential Chair in Science at the University of Oregon. Her research focuses on using spectroscopic and computational methods to understand the chemistry and physics that occurs at complex interfaces that have relevance to important issues in renewable energy, environmental remediation, atmospheric chemistry, and biomolecular interfacial assembly. Her career path prior to her appointment at the University of Oregon in 1985 includes a B.S. from Kansas State University (1975), a Ph.D. from U.C. Berkeley (1980), and an assistant professorship at Bryn Mawr College (1980–85). Richmond is a member of the National Academy of Sciences, the American Academy of Arts and Sciences, a current member of the National Science Board and the 2015 President of the American Association for the Advancement of Science (AAAS).

■ ACKNOWLEDGMENTS

The polyelectrolyte studies described have been supported by the U.S. Department of Energy, Office of Basic Energy Sciences, Division of Materials Sciences and Engineering under award DE-FG02-96ER45557. The surfactant and neat oil/water studies described were supported by the National Science Foundation under award NSF-CHE-065252531.

■ REFERENCES

(1) Voet, D.; Voet, J. G.; Pratt, C. W. *Fundamentals of Biochemistry: Life at the Molecular Level*; Wiley: New York, 2006.
(2) Rebhun, M.; Meir, S.; Laor, Y. Using Dissolved Humic Acid to Remove Hydrophobic Contaminants from Water by Complexation-Flocculation Process. *Environ. Sci. Technol.* **1998**, *32*, 981−986.
(3) Zhang, J.; Li, G.; Yang, F.; Xu, N.; Fan, H.; Yuan, T.; Chen, L. Hydrophobically Modified Sodium Humate Surfactant: Ultra-Low Interfacial Tension at the Oil/Water Interface. *Appl. Surf. Sci.* **2012**, *259*, 774−779.
(4) Abdul, A. S.; Gibson, T. L.; Rai, D. N. Use of Humic-Acid Solution to Remove Organic Contaminants from Hydrogeologic Systems. *Environ. Sci. Technol.* **1990**, *24*, 328−333.
(5) Van Stempvoort, D. R.; Lesage, S.; Novakowski, K. S.; Millar, K.; Brown, S.; Lawrence, J. R. Humic Acid Enhanced Remediation of an Emplaced Diesel Source in Groundwater. 1. Laboratory-Based Pilot Scale Test. *J. Contam. Hydrol.* **2002**, *54*, 249−276.
(6) Kan, A. T.; Tomson, M. B. Ground Water Transport of Hydrophobic Organic Compounds in the Presence of Dissolved Organic Matter. *Environ. Toxicol. Chem.* **1990**, *9*, 253−264.
(7) Chiou, C. T.; Malcolm, R. L.; Brinton, T. I.; Kile, D. E. Water Solubility Enhancement of Some Organic Pollutants and Pesticides by Dissolved Humic and Fulvic Acids. *Environ. Sci. Technol.* **1986**, *20*, 502−508.
(8) Magee, B. R.; Lion, L. W.; Lemley, A. T. Transport of Dissolved Organic Macromolecules and Their Effect on the Transport of Phenanthrene in Porous Media. *Environ. Sci. Technol.* **1991**, *25*, 323−331.
(9) Schlautman, M. A.; Morgan, J. J. Binding of a Fluorescent Hydrophobic Organic Probe by Dissolved Humic Substances and Organically-Coated Aluminum Oxide Surfaces. *Environ. Sci. Technol.* **1993**, *27*, 2523−2532.
(10) Becher, P. *Encyclopedia of Emulsion Technology: Applications*; Marcel Dekker Incorporated: New York, 1985.
(11) Galindo-Alvarez, J.; Kim-Anh, L.; Sadtler, V.; Marchal, P.; Perrin, P.; Tribet, C.; Marie, E.; Durand, A. Enhanced Stability of Nanoemulsions Using Mixtures of Non-Ionic Surfactant and Amphiphilic Polyelectrolyte. *Colloid Surf. A* **2011**, *389*, 237−245.
(12) Michaut, F.; Hebraud, P.; Perrin, P. Amphiphilic Polyelectrolyte for Stabilization of Multiple Emulsions. *Polym. Int.* **2003**, *52*, 594−601.
(13) Perrin, P.; Millet, F.; Charleux, B. Emulsions Stabilized by Polyelectrolytes. *Surfactant Sci. Ser.* **2001**, 363−446.
(14) Urzua, M. D.; Mendizabal, F. J.; Cabrera, W. J.; Rios, H. E. Interfacial Properties of Poly(Maleic Acid-Alt-1-Alkene) Disodium Salts at Water/Hydrocarbon Interfaces. *J. Colloid Interface Sci.* **2005**, *281*, 93−100.
(15) Yuan, W.; Mok, M. M.; Kim, J.; Wong, C. L. H.; Dettmer, C. M.; Nguyen, S. T.; Torkelson, J. M.; Shull, K. R. Behavior of Gradient Copolymers at Liquid/Liquid Interfaces. *Langmuir* **2010**, *26*, 3261−3267.
(16) Beverung, C. J.; Radke, C. J.; Blanch, H. W. Adsorption Dynamics of L-Glutamic Acid Copolymers at a Heptane/Water Interface. *Biophys. Chem.* **1998**, *70*, 121−132.
(17) Rotureau, E.; Leonard, M.; Dellacherie, E.; Durand, A. Amphiphilic Derivatives of Dextran: Adsorption at Air/Water and Oil/Water Interfaces. *J. Colloid Interface Sci.* **2004**, *279*, 68−77.
(18) Tsetska Radeva, e. *Physical Chemistry of Polyelectrolytes*; Marcel Dekker, Inc.: New York, 2001; p 882.
(19) Robertson, E. J.; Beaman, D. K.; Richmond, G. L. Designated Drivers: The Differing Roles of Divalent Metal Ions in Surfactant Adsorption at the Oil-Water Interface. *Langmuir* **2013**, *29*, 15511−15520.
(20) McFearin, C. L.; Beaman, D. K.; Moore, F. G.; Richmond, G. L. From Franklin to Today: Toward a Molecular Level Understanding of Bonding and Adsorption at the Oil-Water Interface. *J. Phys. Chem. C* **2009**, *113*, 1171−1188.
(21) Beaman, D. K.; Robertson, E. J.; Richmond, G. L. From Head to Tail: Structure, Solvation, and Hydrogen Bonding of Carboxylate Surfactants at the Organic-Water Interface. *J. Phys. Chem. C* **2011**, *115*, 12508−12516.
(22) Beaman, D. K.; Robertson, E. J.; Richmond, G. L. Metal Ions: Driving the Orderly Assembly of Polyelectrolytes at a Hydrophobic Surface. *Langmuir* **2012**, *28*, 14245−14253.
(23) Beaman, D. K.; Robertson, E. J.; Richmond, G. L. Ordered Polyelectrolyte Assembly at the Oil-Water Interface. *Proc. Natl. Acad. Sci. U.S.A.* **2012**, *109*, 3226−3231.
(24) Beaman, D. K.; Robertson, E. J.; Richmond, G. L. Unique Assembly of Charged Polymers at the Oil-Water Interface. *Langmuir* **2011**, *27*, 2104−2106.
(25) Richmond, G. L. Vibrational Spectroscopy of Molecules at Liquid/Liquid Interfaces. *Anal. Chem.* **1997**, *69*, A536−A543.
(26) Moore, F. G.; Richmond, G. L. Integration or Segregation: How Do Molecules Behave at Oil/Water Interfaces? *Acc. Chem. Res.* **2008**, *41*, 739−748.
(27) McFearin, C. L.; Richmond, G. L. The Role of Interfacial Molecular Structure in the Adsorption of Ions at the Liquid-Liquid Interface. *J. Phys. Chem. C* **2009**, *113*, 21162−21168.
(28) Robertson, E. J.; Richmond, G. L. Chunks of Charge: Effects at Play in the Assembly of Macromolecules at Fluid Surfaces. *Langmuir* **2013**, *29*, 10980−10989.
(29) Robertson, E. J.; Carpenter, A. P.; Olson, C. M.; Ciszewski, R. K.; Richmond, G. L. Metal Ion Induced Adsorption and Ordering of Charged Macromolecules at the Aqueous/Hydrophobic Liquid Interface. *J. Phys. Chem. C* **2014**, *118*, 15260−15273.
(30) Shen, Y. R. Surface-Properties Probed by 2nd-Harmonic and Sum-Frequency Generation. *Nature* **1989**, *337*, 519−525.
(31) Eisenthal, K. B. Liquid Interfaces Probed by Second-Harmonic and Sum-Frequency Spectroscopy. *Chem. Rev.* **1996**, *96*, 1343−1360.
(32) Guyot-Sionnest, P.; Hunt, J. H.; Shen, Y. R. Sum-Frequency Vibrational Spectroscopy of a Langmuir Film: Study of Molecular Orientation of a Two-Dimensional System. *Phys. Rev. Lett.* **1987**, *59*, 1597−1600.
(33) Miranda, P. B.; Shen, Y. R. Liquid Interfaces: A Study by Sum-Frequency Vibrational Spectroscopy. *J. Phys. Chem. B* **1999**, *103*, 3292−3307.
(34) Somorjai, G. A. The Frontiers of Surface-Structure Analysis. *Surf. Interface Anal.* **1992**, *19*, 493−507.
(35) Lambert, A. G.; Davies, P. B.; Neivandt, D. J. Implementing the Theory of Sum Frequency Generation Vibrational Spectroscopy: A Tutorial Review. *Appl. Spectrosc. Rev.* **2005**, *40*, 103−145.
(36) Richmond, G. L. Molecular Bonding and Interactions at Aqueous Surfaces as Probed by Vibrational Sum Frequency Spectroscopy. *Chem. Rev.* **2002**, *102*, 2693−2724.
(37) Jubb, A. M.; Hua, W.; Allen, H. C. Environmental Chemistry at Vapor/Water Interfaces: Insights from Vibrational Sum Frequency Generation Spectroscopy. *Ann. Rev. Phys. Chem.* **2012**, *63*, 107−130.
(38) Chen, Z.; Shen, Y. R.; Somorjai, G. A. Studies of Polymer Surfaces by Sum Frequency Generation Vibrational Spectroscopy. *Annu. Rev. Phys. Chem.* **2002**, *53*, 437−465.
(39) Yan, E. C. Y.; Fu, L.; Wang, Z.; Liu, W. Biological Macromolecules at Interfaces Probed by Chiral Vibrational Sum Frequency Generation Spectroscopy. *Chem. Rev.* **2014**, *114*, 8471−8498.
(40) Kim, G.; Gurau, M.; Kim, J.; Cremer, P. S. Investigations of Lysozyme Adsorption at the Air/Water and Quartz/Water Interfaces by Vibrational Sum Frequency Spectroscopy. *Langmuir* **2002**, *18*, 2807−2811.

(41) Wang, J.; Buck, S. M.; Chen, Z. Sum Frequency Generation Vibrational Spectroscopy Studies on Protein Adsorption. *J. Phys. Chem. B* **2002**, *106*, 11666−11672.
(42) Fu, L.; Ma, G.; Yan, E. C. Y. In Situ Misfolding of Human Islet Amyloid Polypeptide at Interfaces Probed by Vibrational Sum Frequency Generation. *J. Am. Chem. Soc.* **2010**, *132*, 5405−5412.
(43) Kim, G.; Gurau, M. C.; Lim, S. M.; Cremer, P. S. Investigations of the Orientation of a Membrane Peptide by Sum Frequency Spectroscopy. *J. Phys. Chem. B* **2003**, *107*, 1403−1409.
(44) Chen, X. Y.; Clarke, M. L.; Wang, J.; Chen, Z. Sum Frequency Generation Vibrational Spectroscopy Studies on Molecular Conformation and Orientation of Biological Molecules at Interfaces. *Int. J. Mod. Phys. B* **2005**, *19*, 691−713.
(45) Ye, S.; Nguyen, K. T.; Le Clair, S. V.; Chen, Z. In Situ Molecular Level Studies on Membrane Related Peptides and Proteins in Real Time Using Sum Frequency Generation Vibrational Spectroscopy. *J. Struct. Biol.* **2009**, *168*, 61−77.
(46) Fu, L.; Liu, J.; Yan, E. C. Y. Chiral Sum Frequency Generation Spectroscopy for Characterizing Protein Secondary Structures at Interfaces. *J. Am. Chem. Soc.* **2011**, *133*, 8094−8097.
(47) Wang, J.; Chen, X. Y.; Clarke, M. L.; Chen, Z. Detection of Chiral Sum Frequency Generation Vibrational Spectra of Proteins and Peptides at Interfaces in Situ. *Proc. Natl. Acad. Sci. U.S.A.* **2005**, *102*, 4978−4983.
(48) Paszti, Z.; Wang, J.; Clarke, M. L.; Chen, Z. Sum Frequency Generation Vibrational Spectroscopy Studies of Protein Adsorption on Oxide-Covered Ti Surfaces. *J. Phys. Chem. B* **2004**, *108*, 7779−7787.
(49) Wang, J.; Chen, X. Y.; Clarke, M. L.; Chen, Z. Vibrational Spectroscopic Studies on Fibrinogen Adsorption at Polystyrene/Protein Solution Interfaces: Hydrophobic Side Chain and Secondary Structure Changes. *J. Phys. Chem. B* **2006**, *110*, 5017−5024.
(50) Stokes, G. Y.; Gibbs-Davis, J. M.; Boman, F. C.; Stepp, B. R.; Condie, A. G.; Nguyen, S. T.; Geiger, F. M. Making "Sense" of DNA. *J. Am. Chem. Soc.* **2007**, *129*, 7492−7493.
(51) Walter, S. R.; Geiger, F. M. DNA on Stage: Showcasing Oligonucleotides at Surfaces and Interfaces with Second Harmonic and Vibrational Sum Frequency Generation. *J. Phys. Chem. Lett.* **2010**, *1*, 9−15.
(52) Breen, N. F.; Weidner, T.; Li, K.; Castner, D. G.; Drobny, G. P. A Solid-State Deuterium NMR and Sum-Frequency Generation Study of the Side-Chain Dynamics of Peptides Adsorbed onto Surfaces. *J. Am. Chem. Soc.* **2009**, *131*, 14148−14149.
(53) Weidner, T.; Breen, N. F.; Li, K.; Drobny, G. P.; Castner, D. G. Sum Frequency Generation and Solid-State Nmr Study of the Structure, Orientation, and Dynamics of Polystyrene-Adsorbed Peptides. *Proc. Natl. Acad. Sci. U.S.A.* **2010**, *107*, 13288−13293.
(54) Weidnerw, T.; Castner, D. G. SFG Analysis of Surface Bound Proteins: A Route Towards Structure Determination. *Phys. Chem. Chem. Phys.* **2013**, *15*, 12516−12524.
(55) Yang, P.; Ramamoorthy, A.; Chen, Z. Membrane Orientation of MSI-78 Measured by Sum Frequency Generation Vibrational Spectroscopy. *Langmuir* **2011**, *27*, 7760−7767.
(56) Chen, X.; Wang, J.; Boughton, A. P.; Kristalyn, C. B.; Chen, Z. Multiple Orientation of Melittin inside a Single Lipid Bilayer Determined by Combined Vibrational Spectroscopic Studies. *J. Am. Chem. Soc.* **2007**, *129*, 1420−1427.
(57) Doyle, A. W.; Fick, J.; Himmelhaus, M.; Eck, W.; Graziani, I.; Prudovsky, I.; Grunze, M.; Maciag, T.; Neivandt, D. J. Protein Deformation of Lipid Hybrid Bilayer Membranes Studied by Sum Frequency Generation Vibrational Spectroscopy. *Langmuir* **2004**, *20*, 8961−8965.
(58) Rzeznicka, I. I.; Pandey, R.; Schleeger, M.; Bonn, M.; Weidner, T. Formation of Lysozyme Oligomers at Model Cell Membranes Monitored with Sum Frequency Generation Spectroscopy. *Langmuir* **2014**, *30*, 7736−7744.
(59) Volkov, V.; Bonn, M. Structural Properties of GP41 Fusion Peptide at a Model Membrane Interface. *J. Phys. Chem. B* **2013**, *117*, 15527−15535.
(60) Ye, S. J.; Li, H. C.; Yang, W. L.; Luo, Y. Accurate Determination of Interfacial Protein Secondary Structure by Combining Interfacial-Sensitive Amide I and Amide III Spectral Signals. *J. Am. Chem. Soc.* **2014**, *136*, 1206−1209.
(61) Hu, D.; Yang, Z.; Chou, K. C. Interactions of Polyelectrolytes with Water and Ions at Air/Water Interfaces Studied by Phase-Sensitive Sum Frequency Generation Vibrational Spectroscopy. *J. Phys. Chem. C* **2013**, *117*, 15698−15703.
(62) Liu, G.; Wu, D.; Ma, C.; Zhang, G.; Wang, H.; Yang, S. Insight Into the Origin of the Thermosensitivity of Poly 2-(Dimethylamino)-Ethyl Methacrylate. *ChemPhysChem* **2007**, *8*, 2254−2259.
(63) Kherb, J.; Flores, S. C.; Cremer, P. S. Role of Carboxylate Side Chains in the Cation Hofmeister Series. *J. Phys. Chem. B* **2012**, *116*, 7389−7397.
(64) Kim, J.; Kim, G.; Cremer, P. S. Investigations of Polyelectrolyte Adsorption at the Solid/Liquid Interface by Sum Frequency Spectroscopy: Evidence for Long-Range Macromolecular Alignment at Highly Charged Quartz/Water Interfaces. *J. Am. Chem. Soc.* **2002**, *124*, 8751−8756.
(65) Kett, P. J. N.; Casford, M. T. L.; Yang, A. Y.; Lane, T. J.; Johal, M. S.; Davies, P. B. Structural Changes in a Polyelectrolyte Multilayer Assembly Investigated by Reflection Absorption Infrared Spectroscopy and Sum Frequency Generation Spectroscopy. *J. Phys. Chem. B* **2009**, *113*, 1559−1568.
(66) Windsor, R.; Neivandt, D. J.; Davies, P. B. Adsorption of Sodium Dodecyl Sulfate in the Presence of Poly(Ethylenimine) and Sodium Chloride Studied Using Sum Frequency Vibrational Spectroscopy. *Langmuir* **2001**, *17*, 7306−7312.
(67) Shi, Q.; Ye, S.; Spanninga, S. A.; Su, Y.; Jiang, Z.; Chen, Z. The Molecular Surface Conformation of Surface-Tethered Polyelectrolytes on PDMS Surfaces. *Soft Matter* **2009**, *5*, 3487−3494.
(68) Kim, J.; Cremer, P. S. IR−Visible SFG Investigations of Interfacial Water Structure Upon Polyelectrolyte Adsorption at the Solid/Liquid Interface. *J. Am. Chem. Soc.* **2000**, *122*, 12371−12372.
(69) Windsor, R.; Neivandt, D. J.; Davies, P. B. Temperature and pH Effects on the Coadsorption of Sodium Dodecyl Sulfate and Poly(Ethylenimine). *Langmuir* **2002**, *18*, 2199−2204.
(70) Roger, G. M.; Durand-Vidal, S.; Bernard, O.; Meriguet, G.; Altmann, S.; Turq, P. Characterization of Humic Substances and Polyacrylic Acid: A High Precision Conductimetry Study. *Colloid Surf. A* **2010**, *356*, 51−57.
(71) Eisenberg, H. Thermodynamics and the Structure of Biological Macromolecules - Rozhinkes-Mit-Mandeln. *Eur. J. Biochem.* **1990**, *187*, 7−22.
(72) Sakurai, M.; Imai, T.; Yamashita, F.; Nakamura, K.; Komatsu, T.; Nakagawa, T. Temperature-Dependence of Viscosities and Potentiometric Titration Behavior of Aqueous Poly(Acrylic Acid) and Poly(Methacrylic Acid) Solutions. *Polym. J.* **1993**, *25*, 1247−1255.
(73) Dong, H.; Du, H.; Qian, X. Prediction of pK_a Values for Oligo-Methacrylic Acids Using Combined Classical and Quantum Approaches. *J. Phys. Chem. B* **2009**, *113*, 12857−12859.
(74) Sadeghpour, A.; Vaccaro, A.; Rentsch, S.; Borkovec, M. Influence of Alkali Metal Counterions on the Charging Behavior of Poly(Acrylic Acid). *Polymer* **2009**, *50*, 3950−3954.
(75) Oosawa, F. Counterion Fluctuation and Dielectric Dispersion in Linear Polyelectrolytes. *Biopolymers* **1970**, *9*, 677.
(76) Lin-Vien, D. *The Handbook of Infrared and Raman Characteristic Frequencies of Organic Molecules*; Academic Press: New York, 1991.
(77) Garces, J. L.; Koper, G. J. M.; Borkovec, M. Ionization Equilibria and Conformational Transitions in Polyprotic Molecules and Polyelectrolytes. *J. Phys. Chem. B* **2006**, *110*, 10937−10950.
(78) Freitas, A. A.; Quina, F. H.; Carroll, F. A. Estimation of Water-Organic Interfacial Tensions. A Linear Free Energy Relationship Analysis of Interfacial Adhesion. *J. Phys. Chem. B* **1997**, *101*, 7488−7493.
(79) Hore, D. K.; Walker, D. S.; Richmond, G. L. Layered Organic Structure at the Carbon Tetrachloride-Water Interface. *J. Am. Chem. Soc.* **2007**, *129*, 752−753.

(80) Zhang, J.; Pelton, R. Application of Polymer Adsorption Models to Dynamic Surface Tension. *Langmuir* **1999**, *15*, 5662−5669.
(81) Zhang, J.; Pelton, R. The Dynamic Behavior of Poly(N-Isopropylacrylamide) at the Air/Water Interface. *Colloid Surf. A* **1999**, *156*, 111−122.
(82) Katz, A. K.; Glusker, J. P.; Beebe, S. A.; Bock, C. W. Calcium Ion Coordination: A Comparison with That of Beryllium, Magnesium, and Zinc. *J. Am. Chem. Soc.* **1996**, *118*, 5752−5763.
(83) Oosawa, F. *Polyelectrolytes*; Marcel Dekker, Inc.: New York, 1971.
(84) Rivas, B. L.; Pereira, E. D.; Moreno-Villoslada, I. Water-Soluble Polymer-Metal Ion Interactions. *Prog. Polym. Sci.* **2003**, *28*, 173−208.
(85) Jerman, B.; Kogej, K. Fluorimetric and Potentiometric Study of the Conformational Transition of Isotactic and Atactic Poly-(Methacrylic Acid) in Mixed Solvents. *Acta Chim. Slov.* **2006**, *53*, 264−273.
(86) Jerman, B.; Podlipnik, C.; Kogej, K. Molecular Dynamics Simulation of Poly(Methacrylic Acid) Chains in Water. *Acta Chim. Slov.* **2007**, *54*, 509−516.
(87) Jerman, B.; Breznik, M.; Kogej, K.; Paoletti, S. Osmotic and Volume Properties of Stereoregular Poly(Methacrylic Acids) in Aqueous Solution: Role of Intermolecular Association. *J. Phys. Chem. B* **2007**, *111*, 8435−8443.
(88) Vlachy, N.; Dolenc, J.; Jerman, B.; Kogej, K. Influence of Stereoregularity of the Polymer Chain on Interactions with Surfactants: Binding of Cetylpyridinium Chloride by Isotactic and Atactic Poly(Methacrylic Acid). *J. Phys. Chem. B* **2006**, *110*, 9061−9071.
(89) Raczynska, E. D.; Duczmal, K.; Darowska, M. Experimental (FT-IR) and Theoretical (DFT-IR) Studies of Keto-Enol Tautomerism in Pyruvic Acid. *Vib. Spectrosc.* **2005**, *39*, 37−45.
(90) Robertson, E. J.; Valley, N. A.; Richmond, G. L. Submitted, 2014.
(91) Konradi, R.; Ruhe, J. Interaction of Poly(Methacrylic Acid) Brushes with Metal Ions: An Infrared Investigation. *Macromolecules* **2004**, *37*, 6954−6961.
(92) Sabbagh, I.; Delsanti, M.; Lesieur, P. Ionic Distribution and Polymer Conformation, near Phase Separation, in Sodium Polyacrylate/Divalent Cations Mixtures: Small Angle X-Ray and Neutron Scattering. *Eur. Phys. J. B* **1999**, *12*, 253−260.
(93) Ikegami, A.; Imai, N. Precipitation of Polyelectrolytes by Salts. *J. Polym. Sci.* **1962**, *56*, 133−152.
(94) Konradi, R.; Ruhe, J. Interaction of Poly(Methacrylic Acid) Brushes with Metal Ions: Swelling Properties. *Macromolecules* **2005**, *38*, 4345−4354.
(95) Lages, S.; Michels, R.; Huber, K. Coil-Collapse and Coil-Aggregation Due to the Interaction of Cu^{2+} and Ca^{2+} Ions with Anionic Polyacylate Chains in Dilute Solution. *Macromolecules* **2010**, *43*, 3027−3035.
(96) Ikegami, A. Hydration and Ion Binding of Polyelectrolytes. *J. Polym. Sci., Part A* **1964**, *2*, 907−921.
(97) Schweins, R.; Lindner, P.; Huber, K. Calcium Induced Shrinking of Napa Chains: A Sans Investigation of Single Chain Behavior. *Macromolecules* **2003**, *36*, 9564−9573.
(98) Michaeli, I. Ion Binding and the Formation of Insoluble Polymethacrylic Salts. *J. Polym. Sci.* **1960**, *48*, 291−299.
(99) Ikeda, Y.; Beer, M.; Schmidt, M.; Huber, K. Ca^{2+} and Cu^{2+} Induced Conformational Changes of Sodium Polymethacrylate in Dilute Aqueous Solution. *Macromolecules* **1998**, *31*, 728−733.